REFERENCES

[1] J. D. Rhodes, "A lowpass prototype network for microwave linear phase filters," *IEEE Trans. Microwave Theory Tech.*, vol. MTT-18, pp. 290–301, June 1970.

[2] ——, "The generalized interdigital linear phase filter," *IEEE Trans. Microwave Theory Tech.*, vol. MTT-18, pp. 301–307, June 1970.

[3] ——, "The generalized direct-coupled cavity linear-phase filter," *IEEE Trans. Microwave Theory Tech.*, vol. MTT-18, pp. 308–313, June 1970.

[4] R. Levy, "Filters with single transmission zeros at real or imaginary frequencies," *IEEE Trans. Microwave Theory Tech.*, vol. MTT-24, pp. 172–181, Apr. 1976.

[5] A. E. Atia and A. E. Williams, "Nonminimum-phase optimum-amplitude bandpass waveguide filters," *IEEE Trans. Microwave Theory Tech.*, vol. MTT-22, pp. 425–431, Apr. 1974.

[6] R. Levy, "Mixed lumped and distributed linear phase filters," in *1974 European Conf. on Circuit Theory and Design*, IEE (London), Conf. Publ. no. 116, pp. 32–37.

[7] J. D. Rhodes, "Filters with periodic phase delay and insertion-loss ripple," in *Proc. Inst. Elec. Eng.*, vol. 119, no. 1, pp. 28–32, Jan. 1972.

[8] ——, "Filters approximating ideal amplitude and arbitrary phase characteristics," *IEEE Trans. Circuit Theory*, vol. CT-20, pp. 120–124, Mar. 1973.

[9] R. J. Wenzel, "Solving the approximation problem for narrowband bandpass filters with equal-ripple passband response and arbitrary phase response," in *1975 IEEE MTT-S Int. Microwave Symp.*, IEEE Catalog no. 75CH0955-5, p. 50.

[10] Von K. Wittman, G. Pfitzenmaier, and F. Künemund, "Dimensionierung reflexionsfaktor-und laufzeitgeebneter versteilerter Filter mit Uberbrückungen," *Frequenz*, vol. 24, pp. 307–312, Oct. 1970.

[11] J. H. Cloete, "Microwave linear phase filters," Progress report no. 2, Dept. Electrical Engineering, Univ. Stellenbosch, South Africa, Feb. 1978. (Copies may be obtained from the Head of the Department.)

[12] C. E. Schmidt, "Delay equalizers," *Wescon Digest*, Los Angeles, CA, Aug. 1970.

Band-Limited Deconvolution of Locating Reflectometer Results

PETER I. SOMLO, SENIOR MEMBER, IEEE

Abstract—**The locating reflectometer [1] is a frequency-swept microwave instrument which, by analog Fourier transformation, converts the reflection coefficient, a function of frequency $\Gamma(s)$, into the spatial distribution of the reflection coefficient $\Gamma(x)$. It will be shown that by the method of deconvolution an increase in axial resolution may result. By making use of the fact that the real and imaginary parts of the "locating plot" $\Gamma(x)$ are a Hilbert transform pair, a signal-to-noise ratio improvement is achieved by averaging the results of complex deconvolution using only the real and then only the imaginary parts of the locating plots. A number of experimental results are given, illustrating the increase in axial resolution when the method of band-limited deconvolution is applied to some typical waveguide components and obstacles.**

I. FORMULATION OF THE PROBLEM

LET US assume that we have an instrument, a locating reflectometer[1] (LR) [1], that gives a plot of the distribution of the (complex) reflection coefficient $h(x)$ of a component having a number of internal reflections as a function of distance along the waveguide x. This distribution will be referred to as the "locating vector." Assume that, if more than one reflection is present in the waveguide tested, the instrument will record the *superposition* of these reflections. Because of the bandwidth limitation of the instrument, the locating plot of a single lumped reflection will have some axial spread, since zero spread would require infinite bandwidth. This response to a single lumped reflection we shall call the "instrument function" $g(x)$ which some other workers have referred to as the "pulse response" or the "aperture function." Since we have assumed that the instrument superimposes individual lumped reflection coefficient plots of axial distributions

$$h(x)=\sum_{i=1}^{k}\left[a_i g(x-x_i)\right] \tag{1}$$

i.e., k individual reflection coefficient axial distributions with different complex magnitudes and central positions are added to form the observed locating vector $h(x)$. In other words, we may regard $h(x)$ as the sum of a number of scaled and shifted identical functions. It is well known [2] that the convolution of a function with an impulse function (Dirac function) will duplicate the given function, and, similarly, the convolution of a given function with a number of weighted and shifted impulse functions will produce the sum of the weighted and shifted original functions. Designating the set of weighted and shifted impulse functions as $f(x)$, the observed locating vector is

Manuscript received April 10, 1978; revised July 6, 1978.

The author is with the National Measurement Laboratory, CSIRO, Sydney, Australia 2070.

[1]The locating reflectometer grew out of two reflectometers, the high resolution reflectometer [7] and the comparison reflectometer [8], resulting in an analog instrument with the minimum of electronic circuitry but yielding the values and the locations of individual reflections.

0018-9480/79/0200-0128$00.75 ©1979 IEEE

thus

$$h(x)=f(x)*g(x) \tag{2}$$

where the * denotes convolution. If capitals denote Fourier transforms, then

$$H(s)=F(s)\cdot G(s) \tag{3}$$

indicating that convolving two functions is equivalent to multiplying their Fourier transforms [2].

In the present representation of individual reflections, the effects of multiple reflections have been ignored but will be dealt with in the section on limitations of deconvolution (Section II-A).

If the axial spacing of the individual reflections making up $h(x)$ is closer than the "spread" of an individual reflection's plot, it will not be possible to break down a composite record into its constituents by eye, but with the aid of deconvolution the weighted and shifted impulses representing the magnitudes and locations of the individual reflections may be obtained. So it is $f(x)$ we wish to obtain.

II. The Technique of Deconvolution

If (2) represented the convolution of f and g, then the procedure of obtaining f from h and g may be termed deconvolution. A possible way to obtain f is suggested by (3):

$$F(s)=\frac{H(s)}{G(s)} \tag{4}$$

and via "inverse" Fourier transformation $f(x)$ is obtained.

For the purpose of speeding up the computation of forward and inverse Fourier transforms, the method of the fast Fourier transformation (FFT) has been used. This implies that the functions dealt with are periodic in the interval of investigation. Although this is an approximation, it is evident on inspecting the plots (a) and (b) of Figs. 2–5 that when using a scan of 36 cm, h and g have died down sufficiently at the edges of the interval so that the assumption that it is periodic causes negligible error.

A. Band Limitation

If the LR plots are sampled at regular intervals using n points, then, in general, n complex frequencies are defined. This may suggest that since resolution is limited by the number of harmonics used, which in turn is defined by n, improved resolution should be possible by increasing n.

Dealing with deconvolution in general, we should distinguish between two cases. Using the analogy of magnetic tape recording, in the first case, a video tape recording has been made with information up to 5 MHz. If this tape is played back with a worn head having a widened gap, the high frequencies will be severely attenuated and a "smearing" takes place. In theory, in the absence of noise and with knowledge of the impulse response of the playback head, the full original video content may be restored via deconvolution. In the second case, let us assume that before recording the video message has passed through an ideal low-pass filter cutting everything off above 1 MHz. In this case, no amount of knowledge of the play-back head impulse response will enable us to reconstitute frequency content above 1 MHz, as the information was irretrievably lost before recording.

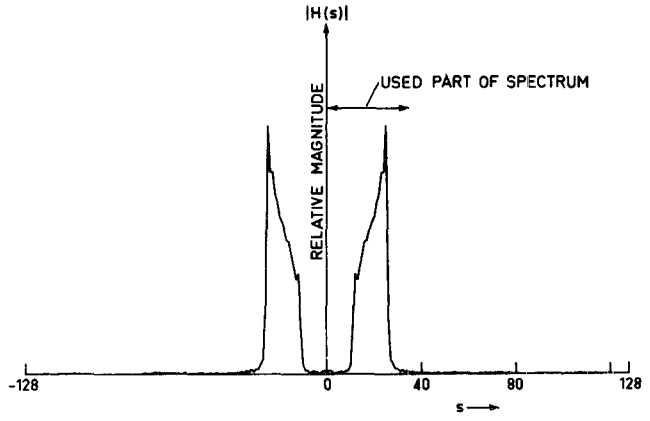

Fig. 1. Magnitude of the computed spectrum of a typical locating reflectometer plot: that of a reflective flange joint. The band-limited nature of the spectrum is evident.

The LR falls in this second category. It is a swept instrument operated in the X band from 8.2 to 12.4 GHz. There is no information available on the behavior of reflection coefficients outside this band, and thus a physical, not a mathematical limitation, is set on the resolution. This is shown in the computed spectra of LR plots. If n is chosen to be 256 and the spectrum of any locating plot is computed using FFT, we find that frequencies corresponding to near 50 GHz are computed. Their value is small but nonzero, because of analog and digital noise. A typical spectrum is shown in Fig. 1. In normal Fourier synthesis, these fictitious frequencies (outside the physically justifiable band) of small amplitudes would cause no trouble. However, in deconvolution when two spectra are divided by each other, the division of one small noisy quantity into another may result in noise which is numerically significant but carries no useful information. For this reason we limit the frequencies used for computation to those within the physically justifiable band and discard the remainder of the spectrum. The number of sample points is still kept large, so that good definition of the used part of the spectrum is obtained due to redundancy (noise averaging). Because only a finite section of the locating plot (extending to infinity) is observed, a slight spreading of the spectrum results, so additional high-frequency components are retained. Due to instrument imperfections (lack of perfect leveling, component frequency responses, etc.), low-frequency components are present on the locating plots, and for this reason it was found beneficial to retain the low-frequency content of the spectrum. Referring to Fig. 1, harmonics up to the thirty second are retained, but above that they are discarded. The value of the highest harmonic used is ob-

tained by calculating the ratio of the distance scanned by the LR to the half-guide wavelength of the highest frequency of the sweep. To this number, an arbitrary constant 8 is added to take in the skirt of the spectrum caused by the truncation of the locating plot.

B. Making Use of Hilbert Transform Pairs

It can be shown [2] that due to causality the real and imaginary parts of either the input impedance or the transfer function of any realizable network are a Hilbert transform pair and are therefore not independent of each other. Each may be generated from the other via Hilbert transformation. One property of Hilbert transformation is that the amplitudes of the spectral components are left unchanged, but their phases are altered by $\pi/2$, positively or negatively according to the sign of the frequency. In the LR this is exactly how the imaginary part is generated from the real part by the use of a 3-dB directional coupler which in the coupled arm, ideally, shifts the phases of all frequency components by 90° relative to the main arm [1]. However, a practical coupler only approximates this condition; the phase shifts will not always be exactly 90°, and the power division will not always be equal. Therefore, a direct complex deconvolution would be hindered by these imperfections. Moreover, the real and imaginary parts are obtained by the use of a separate crystal detector pair and separate amplifiers, and the deconvolution would be affected by differential gains between the real and imaginary outputs. Use will be made of the fact that no extra information is carried by either part relative to the other. It is another property of a Hilbert transform pair that the Fourier spectrum of the pair (one regarded as real, the other imaginary) has no negative frequency components. Therefore, when a measurement is carried out with the LR, both the real and imaginary outputs are data logged, but initially the imaginary parts of h and g are stored and not used. However, the spectra of the complex h and g are calculated by calculating the transforms of Re h and Re g and discarding the negative frequency components. After the division of the remaining (band-limited) spectra, the spectrum of f is available. This result is stored and later averaged with the result obtained in a similar fashion from Im h and Im g only. To illustrate the advantage of the above procedure, suppose that there is a gain difference between the real and imaginary outputs of the LR. Let the ratio of the gains be r. Because

$$F(x)=\frac{\text{Re } H(s)+j \text{ Im } H(s)}{\text{Re } G(s)+j \text{ Im } G(s)} \neq \frac{r \text{ Re } H(s)+j \text{ Im } H(s)}{r \text{ Re } G(s)+j \text{ Im } G(s)} \tag{5}$$

it is indicated that $F(s)$ is obtained only if the gains of the real and imaginary amplifier are equal, i.e., when $r=1$. By similar means it may be shown that for proper deconvolution exact phase quadrature between the parts is required. However, if the quadrature part is obtained by Hilbert transformation, the relative amplitudes and phases of the real and imaginary outputs do not matter, and in the absence of noise the two results of the deconvolutions of corresponding parts would be identical. Because of the duplication of information content in the real and imaginary parts, by logging both in one observation time the unknown is measured twice, and, by averaging, an improvement in the signal-to-noise ratio results. After the division of the spectra the spectrum of f is also that of a Hilbert transform pair (no negative frequencies), so the result of deconvolution is a complex analytic function with the real and imaginary parts in quadrature.

III. Limitations of Deconvolution

There are two main reasons in addition to the inherent bandwidth limitation which limit the accuracy to which nearby waveguide obstacles may be separated by deconvolution. These are 1) lack of superposition of individual reflections and 2) noise enhancement.

A. Lack of Superposition

It has been assumed above that when more than one reflection is present in a component tested, the locating plots will be superpositions of the plots of the individual reflections. This is only an approximation. Consider two loss-free reflections in a waveguide given by their S parameters S' and S''. The input reflection coefficient is

$$\Gamma_{\text{in}}=S'_{11}+\frac{S'^2_{12}S''_{11}\epsilon^{-2j\phi}}{1-S'_{11}S''_{11}\epsilon^{-2j\phi}} \tag{6}$$

which will approximate

$$\Gamma_{\text{in}}\simeq S'_{11}+S''_{11}\epsilon^{-2j\phi} \tag{7}$$

only if $S'_{11}\ll 1$ and $S''_{11}\ll 1$, in which case we have a superposition of two reflections according to (7). The term S'^2_{12} represents the power loss in passing the first reflection, and the second term of the denominator represents multiple reflections. If the two reflections are small, these perturbing effects are small and deconvolution may succeed. The second reason for lack of superposition is caused by the proximity of reflections. Every reflection sets up a set of evanescent modes around it, and if the obstacles are so close that these evanescent fields interact significantly, the two reflections will not superimpose. The first higher mode decays at a rate of about 15.5 dB/cm in X-band waveguide, and at close proximity the higher order modes also become significant. It has been found by experiment that obstacles could not be separated from each other if closer than about 1.5 cm.

B. Noise Enhancement

In the method described here, deconvolution is obtained by the division of two Fourier spectra. If the spectrum of the instrument function g contains local "holes," then dividing by very small numbers can give rise to a magnification. A threshold has been built into the program to detect this magnification, and, if it has occurred, the magnified harmonic is attenuated. In some cases this magnification is justified (i.e., not caused by noise), and there are methods available to deal with the retrieval of the so-called "invisible solutions" [3].

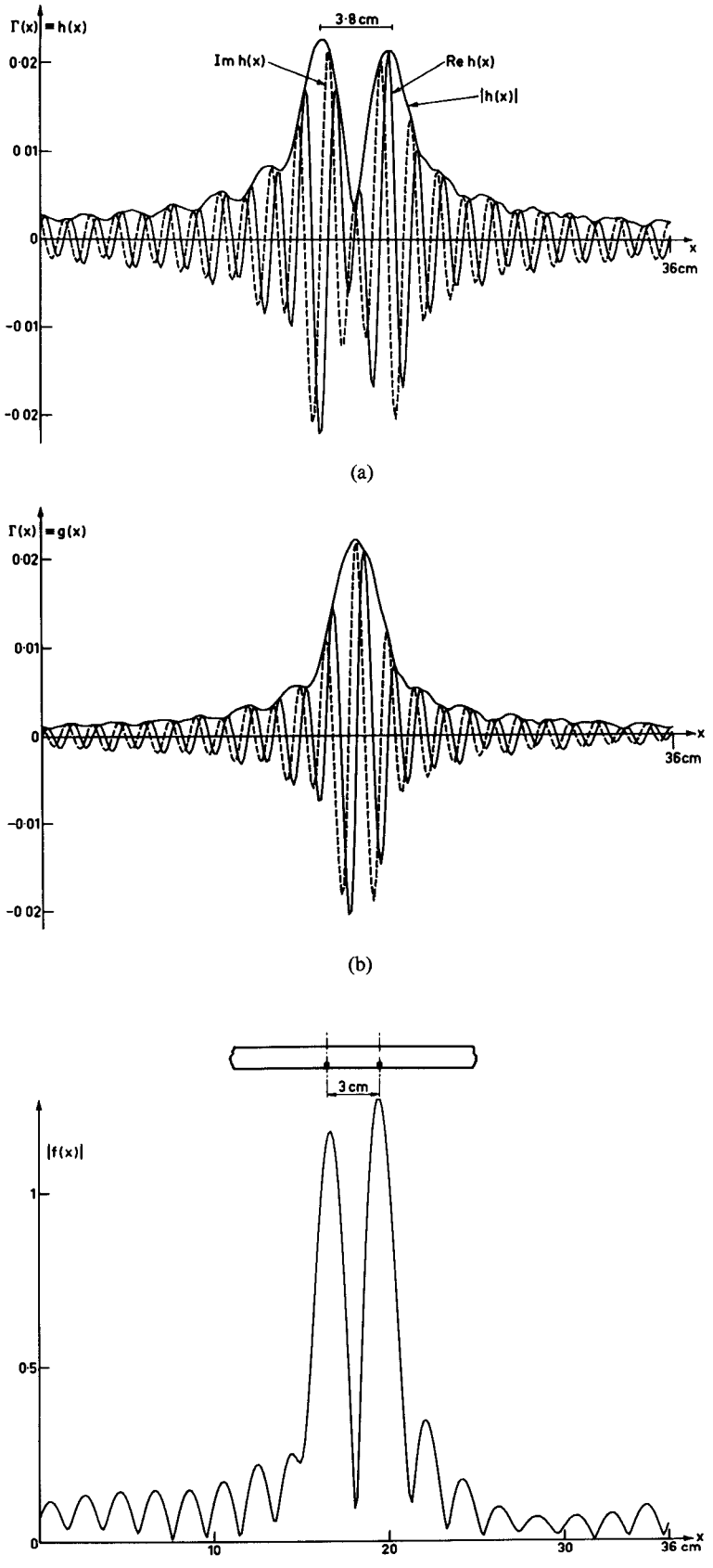

Fig. 2. Deconvolution of a pair of 1.6-mm (1/16-in) diam ball bearings 3 cm apart in an X-band waveguide (a) versus the locating plot of a single ball (b). Deconvolution (c) shows the correct spacing between balls.

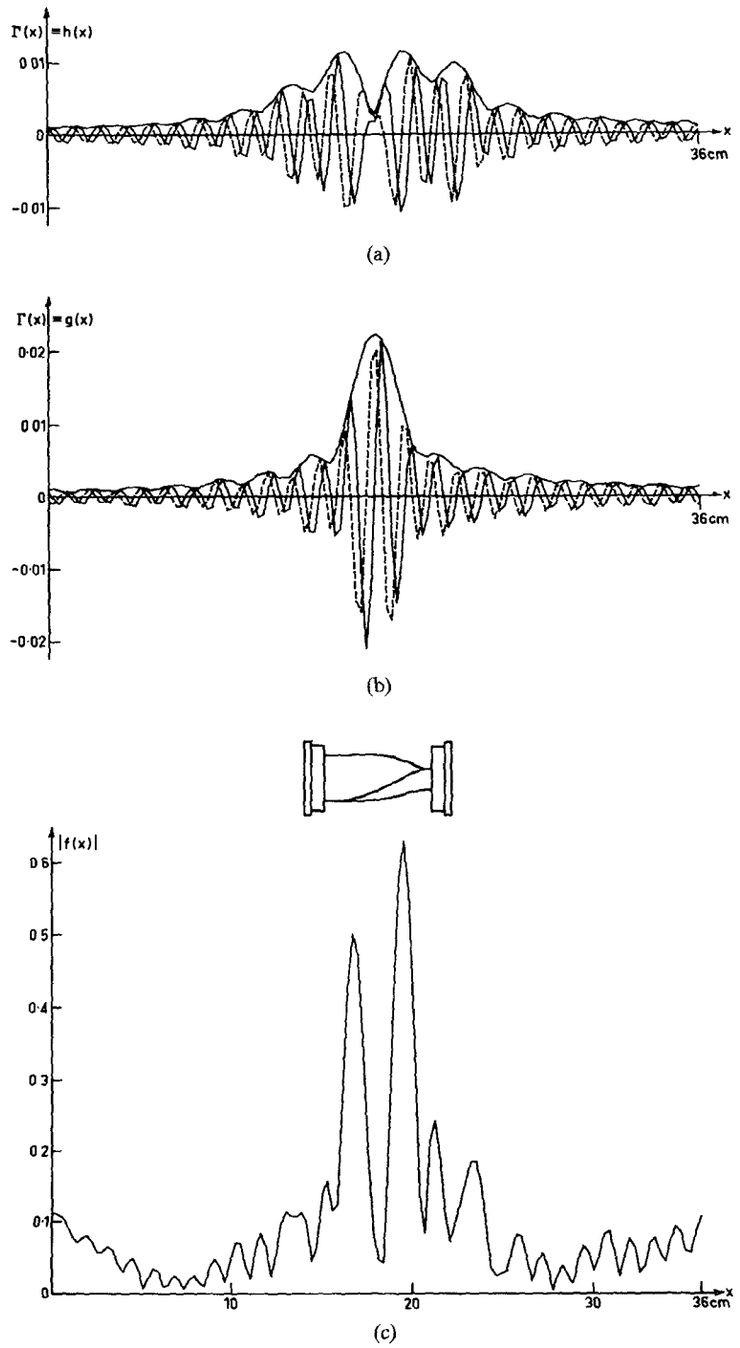

Fig. 3. Deconvolution of the locating plot of a waveguide twist (a) with that of a ball bearing (b), resulting in (c), indicating that the major reflections are located at the ends of the twisted section.

IV. Results

For every attempt at deconvolution an instrument function $g(x)$ is required which for most cases has to be the response to a single lumped reflection. It has been found that a small steel ball (ball bearing) produces a nearly constant reflection coefficient across the waveguide band if placed in the center of the broad wall [4], and, therefore, a small ball shifted and held by an external magnet was used to obtain $g(x)$. The ball was inserted in a long terminated waveguide and was positioned to be in the center of the distance scan examined by the LR. Ball size found most useful was 1.6-mm (1/16-in) diam, resulting in a magnitude of about 0.022 of reflection coefficient. In all the results given here, only the magnitude of the resulting complex answer versus distance along the waveguide is plotted. The results are normalized to the magnitude of the reference reflection used in obtaining the instrument function. Fig. 2 is a test case having two ball

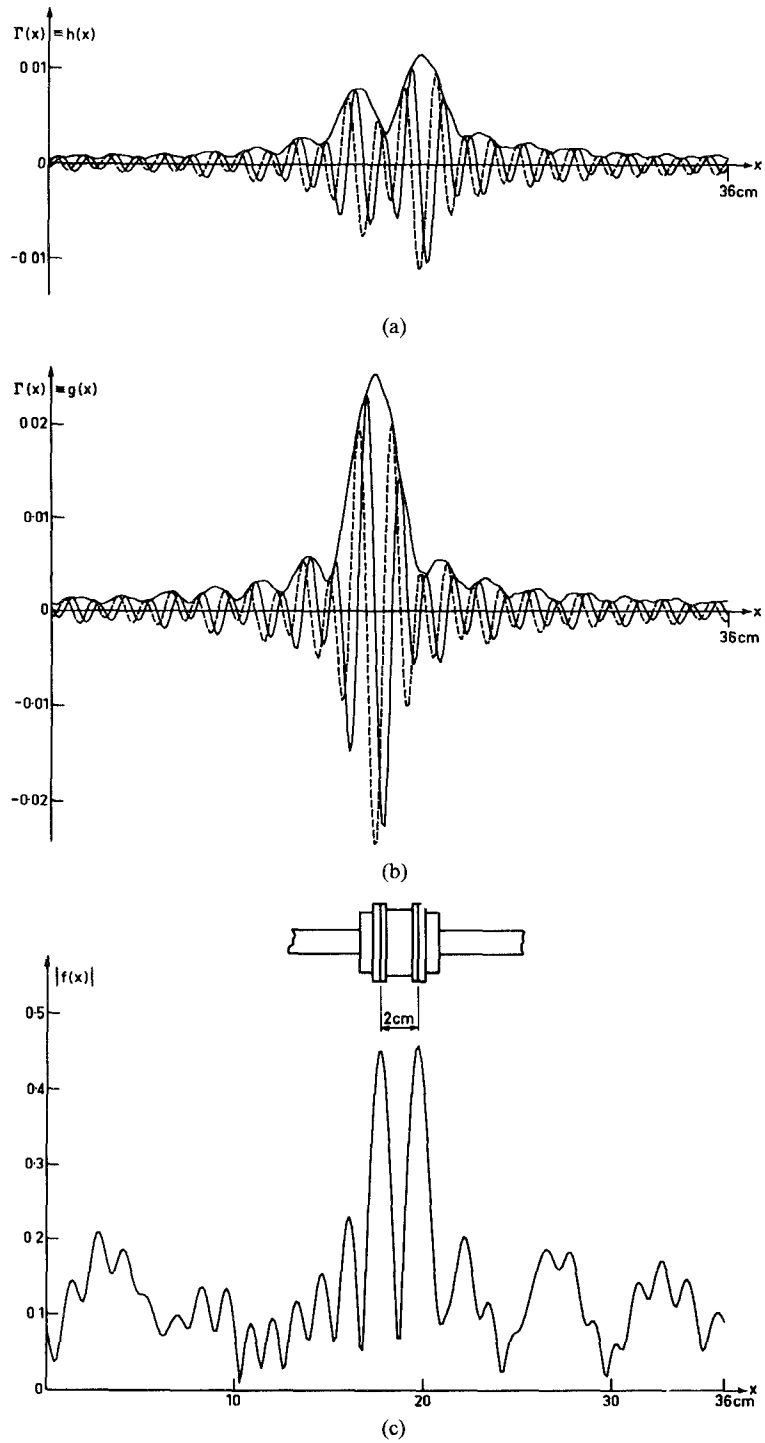

Fig. 4. Deconvolution of the locating plot of a 2-cm long waveguide spacer section (a) with that of a single reflective flange joint (b), resulting in (c), indicating the 2-cm separation of the reflective flange joints.

bearings placed 3 cm ($3/4\lambda_g$ at midband) from each other. As Fig. 2 shows, the locating plot indicates two reflections, but the peaks are 3.8-cm from each other. After deconvolution, Fig. 2(c) shows the two peaks at normalized values near unity, with a separation very close to 3 cm—the correct physical separation of the balls. Fig. 3(a) shows the locating plot of a waveguide 90° twist section. From the locating plot the nature of the reflections is not clear; however, after deconvolution Fig. 3(c) shows that the principal reflections occur at the beginning and at the end of the twist. The physical contours of the waveguide components tested are superimposed on the graphs for comparison. Fig. 4 is the deconvolution of a 2-cm long waveguide spacer section against a single reflective flange joint. The result clearly shows the locations of the flange reflections at a 2-cm separation (c) which was not recog-

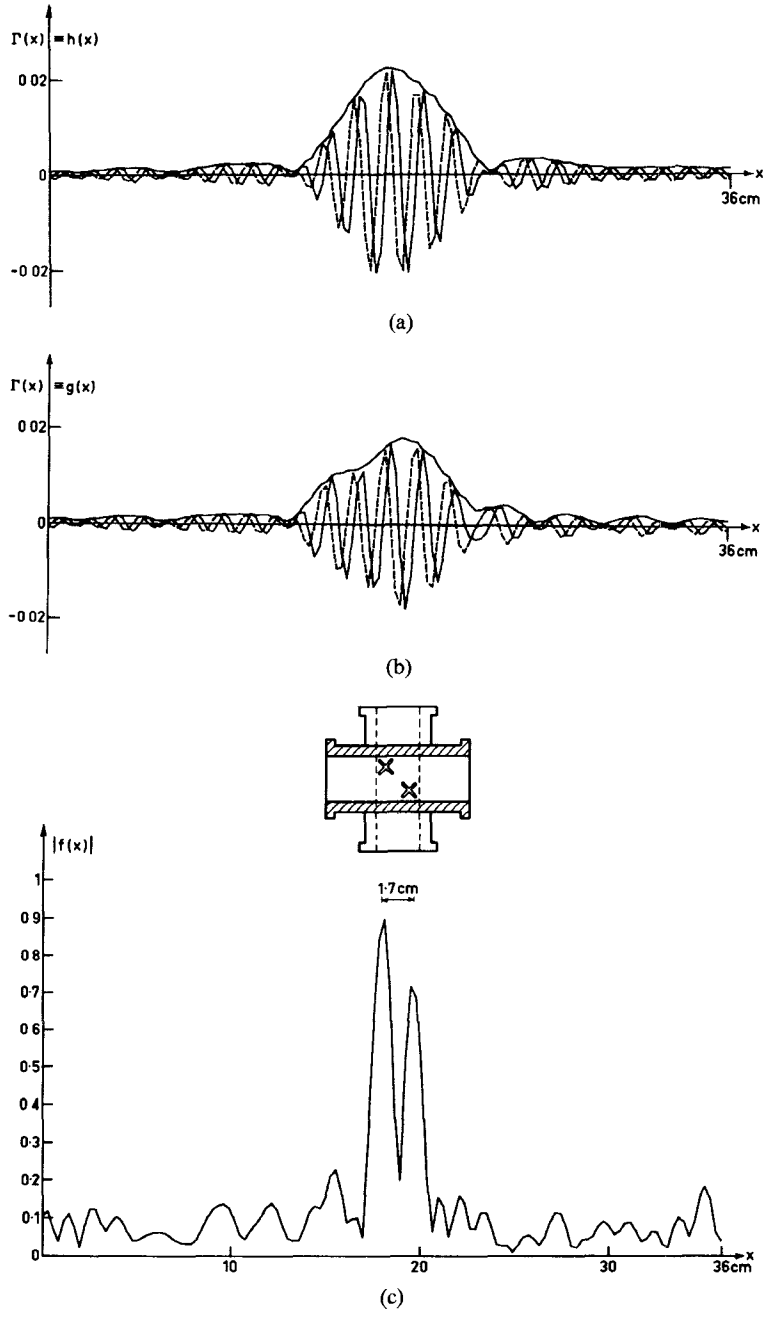

Fig. 5. Deconvolution of the locating plot of a 20-dB cross-guide coupler (a) with the locating plot obtained when one of the two coupling holes was covered up with conductive adhesive tape (b). Deconvolution reveals that the reflections of (a) were made up of two reflections of (b) with an indicated separation of 1.7 cm. The axial separation of the coupling holes is 1.4 cm. In this instance the "instrument function" was a composite structure, and deconvolution reveals the presence of more of these structures.

nizable in the original locating plot (a). Fig. 5 is a special case of deconvolution when the instrument function g was not the response to a single lumped reflection. This is the case of a 20-dB cross-guide coupler. An attempt to deconvolve the locating plot of Fig. 5(a) against a single ball bearing did not result in anything recognizable. However, when one of the two cross-shaped coupling apertures was covered up with adhesive conductive foil, the locating plot of the "one-hole coupler" was recorded (b). Deconvolution with this "instrument function" resulted in Fig. 5(c), clearly showing *two* reflections 1.7 cm apart. The physical, axial separation of the two crosses is about 1.4 cm. This indicates that deconvolution is a method of seeking replicas (shifted and scaled) of the instrument function, which itself may be a complicated structure.

The locating plots of reflections ((a) and (b) of Figs. 2–5) were obtained by using a type of mechanical scanning of [5] where instead of the circularly shaped slotted

section of [1, Fig. 2], an XY recorder was used to pull a sliding, noncontracting short circuit in a uniform section of waveguide. The recorder was moved in equal increments in the axial direction by a computer, and at each position the real and imaginary outputs of the instrument were read by an A to D converter, and later processed when the average of a predetermined number of scans was available. The data logging was performed with a preset, constant level of confidence [6].

V. Summary

It has been shown that the method of deconvolution of the locating reflectometer is basically different from most applications of deconvolution in that the information available is strictly band limited, i.e. high (and low) frequencies are lost in the "recording" and not in the "playback." Although in this case only a modest improvement in resolution may be expected, the results show cases when the effort was worthwhile. Use was made of the fact that the real and imaginary parts of the data, i.e., the locating plots, are a Hilbert transform pair, and thus one measurement resulted in two independent deconvolutions, one obtained from the real, the other from the imaginary parts only. The results are averaged, improving the signal-to-noise ratio. This method makes the results insensitive to gain differences and to the lack of exact phase quadrature between the real and imaginary parts.

References

[1] P. I. Somlo, "The locating reflectometer," *IEEE Trans. Microwave Theory Tech.*, vol. MTT-20, pp. 105–112, Feb. 1972.
[2] R. N. Bracewell, *The Fourier Transform and Its Applications*. New York: McGraw-Hill, 1965.
[3] H. Arsenault and B. Genestar, "Deconvolution of experimental data," *Can. J. Phys.*, vol. 49, pp. 1865–1868, 1971.
[4] P. I. Somlo and D. L. Hollway, "Conductive contacting spheres on the centre of the broad wall of rectangular waveguides," *Electron. Lett.*, vol. 8, p. 507, Oct. 1972.
[5] ——, "Microwave locating reflectometer," *Electron. Lett.*, vol. 5, pp. 468–469, Oct. 1969.
[6] P. I. Somlo, "Automated measurement of noisy voltages with a preset confidence level," *Electron. Lett.*, vol. 13, pp. 234–235, Apr. 1977.
[7] D. L. Hollway and P. I. Somlo, "A high-resolution swept-frequency reflectometer," *IEEE Trans. Microwave Theory Tech.*, vol. MTT-17, pp. 185–188, Apr. 1969.
[8] D. L. Hollway, "The comparison reflectometer," *IEEE Trans. Microwave Theory Tech.*, vol. MTT-15, pp. 250–259, Apr. 1967.

Shot-Noise in Resistive-Diode Mixers and the Attenuator Noise Model

ANTHONY R. KERR, SENIOR MEMBER, IEEE

Abstract—**The representation of a pumped exponential diode, operating as a mixer, by an equivalent lossy network, is reexamined. It is shown that the model is correct provided the network has ports for all sideband frequencies at which (real) power flow can occur between the diode and its embedding. The temperature of the equivalent network is $\eta/2$ times the physical temperature of the diode. The model is valid only if the series resistance and nonlinear capacitance of the diode are negligible. Expressions are derived for the input and output noise temperature and the noise–temperature ratio of ideal mixers. Some common beliefs concerning noise–figure and noise–temperature ratio are shown to be incorrect.**

I. Introduction

In recent years, the need for low-noise mixers, especially in the field of millimeter-wave radio astronomy, has stimulated a considerable amount of research into the theory and design of mixers and mixer diodes. Improved mixer designs have revealed a substantial discrepancy [1] between measured noise performance and that predicted by the simple attenuator noise model of the mixer.

In the attenuator noise model, the mixer is represented as a lossy network whose port-to-port power loss is equal to the mixer conversion loss, and whose physical temperature T_A accounts for the mixer noise. Uncertainty has existed concerning the value of T_A. One widely held belief is that the output noise–temperature ratio[1] t_M of the mixer should be close to unity, from which it follows that T_A is equal to the physical temperature T of the mixer, and that the noise figure of a room-temperature mixer is equal to its conversion loss. An alternative view is that t_M is equal

Manuscript received February 15, 1978; revised May 18, 1978.

The author is with the National Aeronautics and Space Administration, Goddard Space Flight Center, Institute for Space Studies, New York, NY 10025.

[1]The noise–temperature ratio t_M of a mixer is defined as [2] (the available IF output noise power in bandwidth Δf)$\div(kT\Delta f)$, when the mixer and all its input terminations are maintained at ambient temperature T.

0018-9480/79/0200-0135$00.75 ©1979 IEEE